N_2 fluorescence in photoionization of N_2 by 16.3-150 eV photons

J. R. Machacek[1], T. J. Gay[1], J. E. Furst[2], A. L. D. Kilcoyne[3], J. D. Bozek[3], H. Gould[4], M. S. Lubell[5], K. W. McLaughlin[6]
[1]Behlen Laboratory of Physics, University of Nebraska-Lincoln, Lincoln, NE 68588
[2]School of Applied Sciences, University of Newcastle at Ourimbah, Ourimbah NSW 2258, Australia
[3]Advanced Light Source, Lawrence Berkeley National Laboratory, Berkeley, CA 94720
[4]Lawrence Berkeley National Laboratory, Berkeley, CA 94720
[5]City College of New York, New York, NY 10031
[6]Department of Physics and Engineering, Loras College, Dubuque, IA 52004-0178

Using Beamline 10.0.1.2 of the ALS we have made the first narrow-band excitation function measurements of N_2 over a large energy range.

Why

•N_2 is present in stellar atmospheres, comets, aurora and our own atmosphere. Basic data on this system is important.
•Photo-induced excitation functions are sparse over a large energy range for the most basic of N_2 systems, especially above 30 eV.

How

•Linearly-polarized synchrotron radiation incident on an effusive gas jet.
•An optical stack consisting of a linear polarizer at the magic angle, an interference filter and a PMT measured the intensity of the light. The magic-angle polarizer eliminates the effect of excited-target alignment on emitted intensity.
•Incident photon flux was monitored using a calibrated photodiode.
•Chamber pressure was measured with a ion gauge.

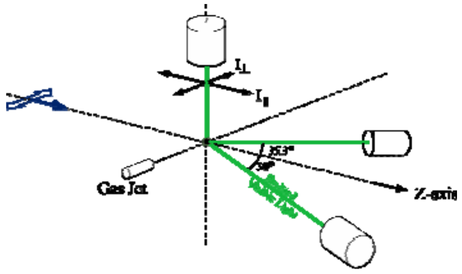

Figure 1: Experimental schematic.

Data Analysis

The background rate was subtracted from the signal rate. This was then normalized to chamber pressure and incident photon flux. Data for each channel of Fig. 2 was taken with an incident photon energy resolution of 10 meV. The uncertainty in Figures 2A and 2B can be seen in the spread of the data. However, due to the low signal obtained the data for Figures 2C and 2D were binned every 100 meV. The error was taken as the standard deviation of the mean of the binned data.

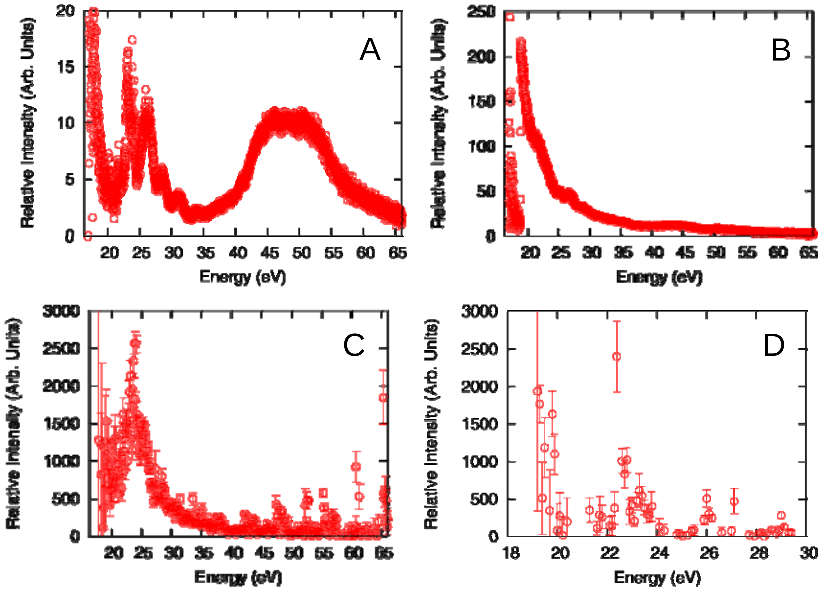

Figure 2: Fluorescence A) 115-200 nm at 144°, B) 375-410 nm at 30°, C) 395-405nm at 35.3° from the z-axis in the plane of the linear polarization of the beam, D) 514.88 nm at 90° from the plane containing the beam and its polarization direction.

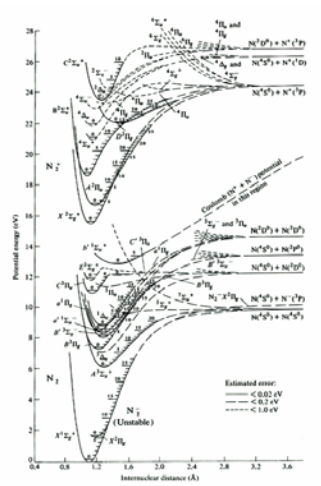

Figure 3: N_2/N_2^+ Potential Curves.

Results and Discussion

Using references [1-3] we constructed a list of observable NI, NII, NIII, N_2, and N_2^+ systems. Fig. 3 was used to rule out any system which was inaccessible due to the incident photon beam energy. References [4,7,8] provided criteria for determining relative intensities between different vibrational transitions. The primary criterion was that transitions from v'=0 dominated in emission over v'=1 [4,7]. Thus, v'>1 transitions were essentially negligible. Table 1 summarizes all observable systems for our apparatus.

Fig. 2A shows five peaks from 20 to 36 eV and a broad peak from approximately 41 to 56 eV. This broad peak is in qualitative agreement with Ehresmann *et al*. [9]

Fig. 2B has a sharp turn-on at 18.81 eV which corresponds to the $B^2\Sigma_u^+$-$X^2\Sigma_g^+$, v'=0 to v'=0 transition.

Filter BW (Å)	Line (Å)	State	v'- v''	Threshold (eV)	System/Band Name
1150-2000	1160- -1200	NI		20.09-41.99	26 Lines
3750-4100	3914.4	$B^2\Sigma_u^+$-$X^2\Sigma_g^+$	0-0	18.6	1st Negative System
	3884.3		1-1	19.1	
	3915	$^4\Sigma_u^+$-$X^4\Sigma_g^+$	0-0	21.15	d'Incan-Topouzkhanian System
	3885		1-1		
	4099.951- -3818.27	NI		~23.72	16 Lines
	4097.3- -3829.793	NII		~45.95	28 Lines
	4097.31- -3752.65	NIII		~84.42	16 Lines
3950-4050	3994.9	$B^2\Sigma_u^+$-$X^2\Sigma_g^+$	22-18	23.0	1st Negative System
	4006.7	$B^2\Sigma_u^+$-$X^2\Sigma_g^+$	20-17	22.8	1st Negative System
	4010.99- -3969.95	NI		~23.6	5 Lines
	3994.998	NII		~45.95	
	4003.64	NIII		~96.46	
	3998.69				
5137.5-5155.0	5148.8	$B^2\Sigma_u^+$-$X^2\Sigma_g^+$	1-4	19.1	1st Negative System

Table 1: Observable lines of the photofragments and their corresponding pertinent properties.

Fig. 2C corresponds to a narrower band without the 391.44 nm transition. There is not a sharp turn-on, but the data have a similar shape after the peak. Small peaks at higher energy could be due to atomic nitrogen thresholds.

Fig. 2D. Singling out the $B^2\Sigma_u^+$-$X^2\Sigma_g^+$, v'=1 to v''=4 molecular transition yields a sharp turn-on at 22.4 eV, but the intensity is very low and near the threshold of our detection capability.

Acknowledgements:

We would like to thank Bruce Rude, the machine shop staff, and the surveying staff of the ALS. We would also like to thank Dr. Duane Jaecks and Dr. Orhan Yenen for helpful discussions. This work was supported by NSF grants PHY-0354946, PHY-00985445, and PHY-0321055.

References:

1. Lofthus, J. Phys. Chem. Ref. Data **6,** 1 (1977).
2. R. W. B. Pearse and A. G. Gaydon, *The Identification of Molecular Spectra*, (John Wiley & Sons, Inc., New York, 1976), 4th ed.
3. A. R. Striganov and N. S. Sventitskii, *Tables of Spectral Lines of Neutral and Ionized Atoms*, (IFI/Plenum, New York,-Washington, 1968).
4. D. L. Judge and G. L. Weissler, J. Chem. Phys. **48**, 4590 (1968).
5. P. Erman, A. Karawajczyk, E. Rachlew-Källne, S. L. Sorensen, C. Strömholm and M Kirm, J. Phys. B **26,** 4483 (1993).
6. M. Kitajima, M. Ukai, S. Machida, K. Kameta, N. Kouchi, Y. Hatano, T. Hayaishi and K. Ito, J. Phys. B **28,** L185 (1995).
7. Wm. B. Peatman, B. Gotchev, P. Gurtler, E. E. Koch, V. Saile, J. Chem. Phys. **69**, 1321 (1978).
8. J. A. Guest, K. H. Jackson, and R. N. Zare, Phys. Rev. A **28,** 2217 (1983).
9. A. Ehresmann, S. Machida, M. Kitajima, M. Ukai, K. Kameta, N. Kouchi, Y. Hatano, E. Shigemasa, and T. Hayaishi, J. Phys. B. **33**, 473 (2000).